Pergamon

Solid State Communications, Vol. 92, No. 7, pp. 601–605, 1994
Elsevier Science Ltd
Printed in Great Britain
0038–1098/94 $7.00 + .00

0038–1098(94)00536–2

MAGNETIC STRUCTURE OF THE CHAIN Mn(III) FLUORIDE Na_2MnF_5

P. Núñez*

Departamento de Química Inorgánica, Universidad de La Laguna, 38200 La Laguna, Canary Islands, Spain

T. Roisnel

Laboratoire Leon Brillouin (CEA-CNRS), CE-Saclay, 91191 Gif-Sur-Yvette Cedex, France

and

A. Tressaud

Laboratoire de Chimie du Solide du CNRS, Université de Bordeaux I, 33405 Talence Cedex, France

(*Received* 10 *May* 1994; *in final form* 28 *June* 1994 *by F. Yndurain*)

The chain Mn(III) fluoride Na_2MnF_5 has been studied by means of neutron powder diffraction. Below $T_N = 11.1(5)$ K, a 3D intrachain antiferromagnetic coupling is observed: this is the first time that a 3D ordering is unambiguously found in anhydrous A_2MnF_5 series. Additionally a magnetic frustration phenomenon is found for the interchain ordering. At 1.5 K the magnetic structure is colinear, with the manganese magnetic moments ($3.3(1)\,\mu_B$) parallel to the a axis. Structural and magnetic data of Na_2MnF_5 are compared with those of other related compounds.

Keywords: magnetic structure, Mn(III) fluoride, linear antiferromagnet, magnetic frustration.

1. INTRODUCTION

$A_2MnF_5.xH_2O$ ($x = 0$, 1; A = monovalent cation) compounds are characterized by infinite chains of $[MnF_6]$ octahedra sharing trans vertices. The $[MnF_6]$ octahedra are axially elongated due to the Jahn–Teller configuration of d^4 Mn(III). The $(MnF_5)_n^{2n-}$ chains are separated by the monovalent cations. Two structural classes have been considered depending on the packing of the chains [1]. In one class a tetragonal arrangement is found, as for instance in Rb_2MnF_5 [2], and in the other one a pseudohexagonal packing is observed for $((NH_4)_2MnF_5$ [3], $BaMnF_5.H_2O$ [4]. Among the latter type of fluorides the structural features of Na_2MnF_5 have been determined by Massa [1] using single crystal X-ray diffractometry. We have previously investigated both high temperature magnetic behaviour and low temperature magnetic ordering of several of these pentafluoromanganates(III) and we have correlated the intrachain exchange constant J/k values to the structural characteristics [5, 6]. In the present work we describe the magnetic structure of Na_2MnF_5. The magnetic properties are compared with those of other A_2MnF_5 compounds.

2. EXPERIMENTAL PROCEDURE

Na_2MnF_5 was prepared by adding solid Mn_2O_3 to a saturated solution of NaF in HF 40% in a similar way to the method described by Massa [1]. The resulting microcrystalline solid was checked by X-ray diffraction.

Neutron powder diffraction measurements were performed at Orphee reactor (CE-Saclay, France), for the structural part at room temperature on the high resolution powder diffractometer D1A ($\lambda = 1.9845$ Å) and for the magnetic study in the 50 to 1.5 K temperature range on the 2-axis diffractometer G4.1 ($\lambda = 2.426$ Å), equipped with an 800-cells position sensitive detector. The data were analysed with Rietveld-type FULLPROF program

* To whom the correspondence should be addressed.

Table 1. Cell parameters, atomic positions and Mn–F *distances of* Na_2MnF_5 *determined from neutron powder diffraction at room temperature*

$a = 7.7197(2)$ Å; $b = 5.2402(2)$ Å; $c = 10.8706(3)$ Å; $\beta = 108.991(3)°$; S.G.: $P2_1/c(14)$

Atom	Site	x	y	z	B_{iso}(Å^2)
Na1	(4e)	0.1535(12)	−0.0107(15)	0.3647(8)	1.58(19)
Na2	(4e)	0.3441(12)	0.4439(17)	0.1796(8)	1.74(19)
Mn1	(2a)	0.	0.	0.	0.68(22)
Mn2	(2b)	0.5	0.	0.	0.69(24)
F1	(4e)	0.0448(7)	0.1510(9)	0.1629(5)	1.78(12)
F2	(4e)	−0.1083(7)	0.2978(10)	−0.0758(5)	1.85(12)
F3	(4e)	0.2514(8)	0.1620(9)	0.0031(5)	1.33(11)
F4	(4e)	0.6179(6)	0.2192(10)	0.1347(4)	1.47(11)
F5	(4e)	0.4918(7)	0.2442(10)	−0.1228(5)	1.65(11)

Mn–F distances

2 × Mn1–F1: 1.866(5) Å;	2 × Mn2–F3: 2.108(7) Å;	2 × Mn1–F2: 1.834(5) Å;
2 × Mn2–F4: 1.850(5) Å;	2 × Mn1–F3: 2.108(7) Å;	2 × Mn2–F5: 1.835(5) Å

[7], using neutron scattering lengths from [8] and Mn^{3+} magnetic form factor from [9].

Magnetic measurements of Na_2MnF_5 were carried out from 2 to 300 K for powdered samples using a SQUID magnetometer. Magnetic fields were applied up to 3 T at low temperature (2 K).

3. RESULTS AND DISCUSSION

3.1. *Nuclear structure*

The atomic positions and the Debye–Waller thermal factors of Na_2MnF_5 (Table 1) were determined from Rietveld profile refinement of neutron diffraction data at room temperature, with reliability factors [10] Rp = 5.8% and Rwp = 7.0% (Fig. 1). The structural data are in good agreement with those obtained by single crystal X-ray diffraction analysis [1].

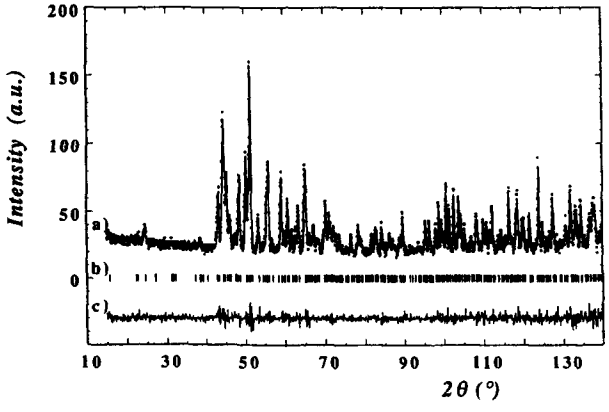

Fig. 1. Neutron diffraction pattern of Na_2MnF_5 at room temperature (a) full circles: experimental points; continuous line: calculated profile; (b) position of the nuclear peak; (c) difference pattern.

Na_2MnF_5 crystallizes in a monoclinic symmetry $P2_1/c$ space group (no. 14), with the cell parameters given in Table 1. There are two non-equivalent manganese atoms located in special positions (2*a* and 2*b*), whereas the other atoms are located in general positions (4*e*).

The $[MnF_6]$ octahedra share two trans corners and are elongated. This axial distortion, with four short Mn–F distances and two long ones, is due to the strong Jahn–Teller effect of the Mn^{3+} ion in a high spin configuration d^4.

The structure of Na_2MnF_5 can be considered as formed by zig-zag infinite chains of octahedra running parallel to the *a* axis, with an intrachain Mn–F–Mn angle of 132°, in such a way that they form a pseudohexagonal packing of chains [1]. Sodium ions are placed between the $(MnF_5)_n^{2n-}$ chains in order to retain the electroneutrality of the compound.

3.2. *Magnetic properties*

The temperature dependence of the reciprocal susceptibility of a powder sample of Na_2MnF_5 is given in Fig. 2. A broad minimum is observed at about 50 K, which is the signature of the 1-D short range antiferromagnetic interactions within the chains and above 80 K this phase obeys a Curie–Weiss law with $C_m = 3.1(1)$ and $\theta_p = -98(8)$ K. The exchange constant within the chains has been calculated by fitting the experimental results to the Fisher model of finite linear chains with a $S = \frac{5}{2}$ spin value and an isotropic Heisenberg Hamiltonian

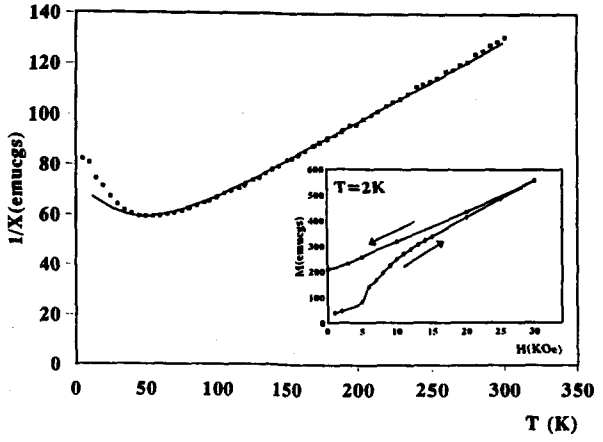

Fig. 2. Magnetic susceptibility of Na_2MnF_5 as a function of the temperature. In the inset, the magnetization vs magnetic field is plotted.

[11, 12]. We have obtained a J/k value of -8.6 K with $g = 1.95$, in good agreement with the values estimated by Emori *et al.* [13] ($J/k = -9.2$ K and $g = 1.97$) and Pebler *et al.* [14] ($J/k = -8.3$ K and $g = 1.84$).

The variation of the magnetization with the magnetic field at 2 K is given in the inset of Fig. 2, where an irreversible field-induced transition is observed. As is obviously shown in this inset, the saturated magnetization is far to be reached, at least for both temperature (2 K) and magnetic field (3 T) used during the experiment.

3.3. *Magnetic structure*

As can be deduced from Fig. 3 the neutron diffraction pattern at 50 K exhibits only nuclear contribution. The unit cell parameters at this temperature are: $a = 7.679(2)$ Å; $b = 5.206(1)$ Å; $c = 10.803(2)$ Å; $\beta = 108.9(1)°$. The neutron powder diffraction pattern at 1.5 K (Fig. 3) shows several

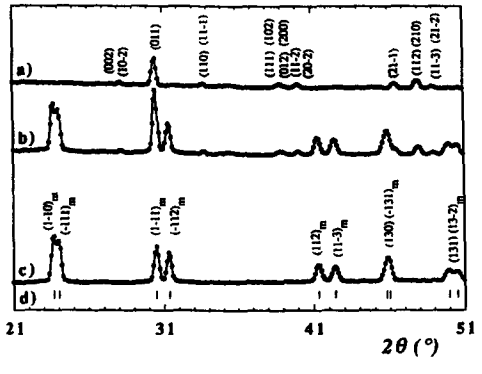

Fig. 3. Neutron diffraction patterns of Na_2MnF_5 at 50 K (a) and 1.4 K (b); difference profile (c) and positions of the magnetic Bragg peaks (d) [the $(hkl)_m$ indexation is given in the magnetic unit-cell].

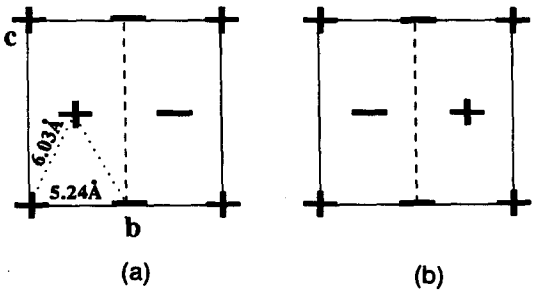

Fig. 4. Schematic representation of the magnetic moment signs of *2a* site in the (*bc*) plane for model *1* (a) and model *2* (b). The *2b* sites can be obtained by a (*1/2, 0, 0*) translation with the opposite signs.

magnetic superstructure Bragg peaks, which cannot be indexed in the nuclear cell, but in a twofold chemical cell (*a2bc*). These superstructure peaks can also be labelled as satellites of nuclear peaks with the propagation vector $k = (0, 1/2, 0)$.

The crystallographic positions for the magnetic atoms in the chemical cell are the following:

2a sites: Mn1: $(0,0,0)$; Mn2: $(0,1/2,1/2)$,

2b sites: Mn3: $(1/2,0,0)$; Mn4: $(1/2,1/2,1/2)$,

each manganese atom possessing Mi ($i = 1$ to 4) spin magnetic moment.

The observed magnetic Bragg peaks correspond to the selection rules: $h = 2n \pm 1$ and $k = 2n \pm 1$, leading to an antiferromagnetic ordering between atoms in (*2a*) and (*2b*) sites. The arrangement within the chains is antiferromagnetic, with two possible equivalent magnetic models:

	M1	M2	M3	M4
Model *1*	+	+	−	−
Model *2*	+	−	−	+

In model *1*, there is a ferromagnetic arrangement between Mn1 and Mn2, both atoms being in the same

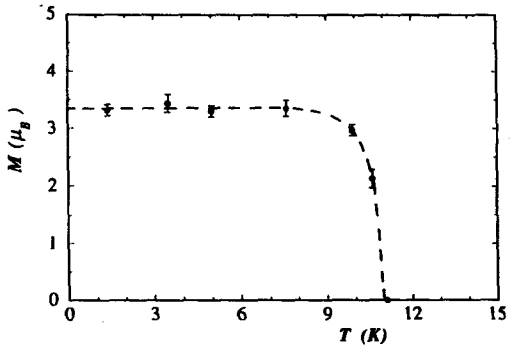

Fig. 5. Thermal variation of the magnetic moment of Mn(III) in Na_2MnF_5.

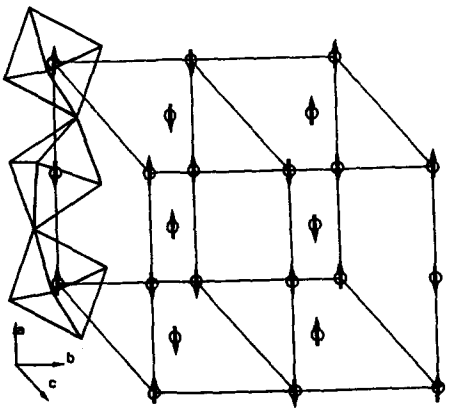

Fig. 6. Magnetic structure of Na_2MnF_5.

crystallographic site, whereas in model *2* there is an antiferromagnetic arrangement within each site. In Fig. 4 both models are schematized in the (*bc*) plane perpendicular to the chains. It can be noted that these two models can be deduced one from another by a (*0, 1/2, 1/2*) translation.

Refinement of the neutron data at $T = 1.5\,K$ leads to a colinear antiferromagnetic structure with the magnetic moment direction along the *a* axis. The thermal variation of the magnetic moment modulus is shown in Fig. 5, leading to a Neel temperature of $T_N = 11.1(5)\,K$. At 1.5 K, the magnetic moment modulus is found to be equal to $3.3(1)\,\mu_B$, which is in good agreement with the expected value for a $S = 2$ ion. The magnetic structure is shown in Fig. 6: the shortest interchain distance (5.24 Å) is found along the *b* axis, which implies a preferential antiferromagnetic ordering in this direction. The second next neighbour chains are separated by 6.03 Å (M1–M2 distance).

3.4. *Discussion*

From the above structural data, it is clear that a magnetic frustration phenomenon [15] originates from the resulting triangular configuration of the $(MnF_5)_n^{2n-}$ chains and explains the two possible models. This magnetic frustration phenomenon is probably responsible for the irreversible field-induced transition observed in the magnetization vs magnetic field curve (Fig. 2, inset).

In $Tl_2MnF_5.H_2O$ [6] a distorted tetragonal packing of chains is observed and the manganese atoms are located at the corners of a rhombus of 6.28 Å edge and 79.1° angle with the shortest interchain distance equal to the edge: each $(MnF_5)_n^{2n-}$ chain is surrounded by four other chains at a same distance. A similar "isotropic" arrangement it has been found in A_2MnF_5 compounds (A = Rb, Cs, NH_4). On the other hand, in Na_2MnF_5 (pseudohexagonal packing) the manganese atoms are also situated at the corners of a rhombus of 6.03 Å edge and 51.5° angle but the shortest interchain distance corresponds to the short diagonal (5.24 Å) in the lozenge. This configuration leads to a doubling of the *b* axis, as shown in Fig. 6. Therefore, at low temperature, the preferential interchain interactions take place between $(MnF_5)_n^{2n-}$ chains contained in planes perpendicular to the *c* axis. These planes are more loosely coupled along the *c* direction.

Magnetic and structural data of Na_2MnF_5 are compared in Table 2 with those of other A_2MnF_5 compounds and $Tl_2MnF_5.H_2O$. Within the A_2MnF_5 series a 3D ordering temperature has been unambiguously found for the Na compound only. For Li_2MnF_5 no ordering could be detected down to 1.5 K and contradictory results have been announced for the ammonium compounds. For the other phases the experiments remain to be done [14, 16].

It has been previously emphasized the relationships between the intrachain exchange constant *J*/

Table 2. Magnetic and structural data of the A_2MnF_5 *series and* $Tl_2MnF_2.H_2O$

Compound	θ_p (K)	T_N (K)	J/k (K)	J'/J[a]	Ref.	Mn–F–Mn (°)[b]	Mn–Mn (Å)[c]	Re
Li_2MnF_5	−66	< 1.5	−6.1	$< 10^{-3}$	14	121.5	4.9 (×2)	14
Na_2MnF_5	−98	11.5	−8.6	$\approx 3 \times 10^{-2}$	[d]	132.5	5.2 (×2)	1
Rb_2MnF_5	−400	?	−22.6	?	5	180	6.1 (×4)	21
Cs_2MnF_5	−345	?	−19.4	?	5	180	6.4 (×4)	22
$(NH_4)_2MnF_5$	−153	?	−10.6	?	14	143.4	6.2 (×6)	3
$Tl_2MnF_5.H_2O$	−470	28	−21.5	$\approx 2 \times 10^{-2}$	6	179	6.3 (×4)	6

[a] Oguchi's method.
[b] Intrachain angle.
[c] Closest interchain distance. In bracket number of distances.
[d] This work.

and the Mn–F–Mn interchain superexchange angle [14]. The value $J/k = -8.6$ K determined for Na_2MnF_5 is in good agreement with the corresponding Mn–F–Mn angle within the series (see Table 2). The ratio interchain-to-intrachain exchange constant $|J'/J|$ may be estimated using several methods. In particular following Oguchi, a relation between $kT_N|J|S(S+1)$ and $|J'/J|$ can be raised [17]. From the estimated value $J'/J \approx 3 \times 10^{-2}$ obtained for Na_2MnF_5, we can assess that there is a balance between the distortion degree of the chain (Mn–F–Mn angle) and the interchain distance (Mn–Mn distance).

Finally, we note that the value of the manganese magnetic moment (3.3 μ_B) is lower than that expected for $S = 4/2$ Mn^{3+} ions. This result is in good agreement with the trend observed in other 1D antiferromagnets [18, 19]. This behavior is attributable to zero-point spin reduction which has been predicted to reduce the ground state spin expectation value in antiferromagnetic systems. This effect can be considered as a result of the zero-point energy of the spin waves destroying any long-range order [20].

REFERENCES

1. W. Massa, *Acta Cryst.* **C42,** 644 (1986).
2. P. Bukovec & V. Kaucic, *Acta Cryst.* **B34,** 339 (1978).
3. D.R. Sears & J.L. Hoard, *J. Chem. Phys.* **50,** 1066 (1969).
4. W. Massa & V. Burk, *Z. Anorg. Allg. Chem.* **516,** 119 (1984).
5. P. Núñez, J. Darriet, P. Bukovec, A. Tressaud & P. Hagenmuller, *Mat. Res. Bull.* **22,** 661 (1987).
6. P. Núñez, A. Tressaud, J. Darriet, P. Hagenmuller, G. Hahn, G. Frenzen, W. Massa, D. Babel, A. Boireau & J.L. Soubeyroux, *Inorg. Chem.* **31,** 770 (1992).
7. J. Rodríguez-Carvajal, *Powder Diffraction Satellite Meeting of XV Congress of IUCr,* Toulouse (France) abs. p. 127 (1990).
8. V.F. Sears, *Neutron News* **3(3),** 26 (1992).
9. P.J. Brown, *International Tables for Crystallography* (Edited by A.J.C. Wilson), Vol. C, table 4.4.4. Kluwer, Dordrecht (1993).
10. Reliability factors were calculated as:

$$Rp = 100\frac{\Sigma|Y^i_{obs} - Y^i_{cal}|}{\Sigma|Y^i_{obs}|}, \text{ and}$$

$$Rwp = 100\left[\frac{\Sigma w_i|Y^i_{obs} - Y^i_{cal}|^2}{\Sigma w_i|Y^i_{obs}|^2}\right]^{1/2}$$

where Y^i_{obs} and Y^i_{cal} are observed and calculated intensity for the point i, respectively. The weighted factor w_i was calculated as $w_i = 1/\sigma(Y^i_{obs})$, where $\sigma(Y^i_{obs})$ is the variance of the Y^i_{obs}.

11. M.E. Fisher, *Amer. J. Phys.* **32,** 343 (1964).
12. T. Smith & S.A. Friedberg, *Phys. Rev.* **176,** 660 (1968).
13. S. Emori, M. Inoue, M. Kishita & M. Kubo, *Inorg. Chem.* **8,** 1385 (1969).
14. J. Pebler, W. Massa, H. Lass & B. Ziegler, *J. Solid State Chem.* **71,** 87 (1987).
15. G. Ferey, M. Leblanc, R. de Pape & J. Pannetier, in *Inorganic Solid Fluorides* (Edited by P. Hagenmuller), p. 395. Academic Press, Orlando (1985).
16. F. Palacio & M.C. Morón, in *Research Frontiers in Magnetochemistry* (Edited by C.J. O'Connor), p. 227. World Scientific, Singapore (1993).
17. T. Oguchi, *Phys. Rev.* **133A,** 1098 (1964).
18. A. Tressaud & J.M. Dance, *Structure and Bonding* **52,** 87 (1982).
19. G.P. Gupta, D.P.E. Dickson, C.F. Johnson & B.M. Wanklyn, *J. Phys. C: Solid State Phys.* **10,** L459 (1977).
20. T. Ishikawa & T. Oguchi, *Prog. Theor. Phys.* **54,** 1282 (1975).
21. J.R. Günther, J.P. Matthieu & H.R. Oswald, *Helv. Chim. Acta* **61,** 328 (1978).
22. F. Hahn & W. Massa, *Z. Naturforsch.* **45b,** 1341 (1990).